

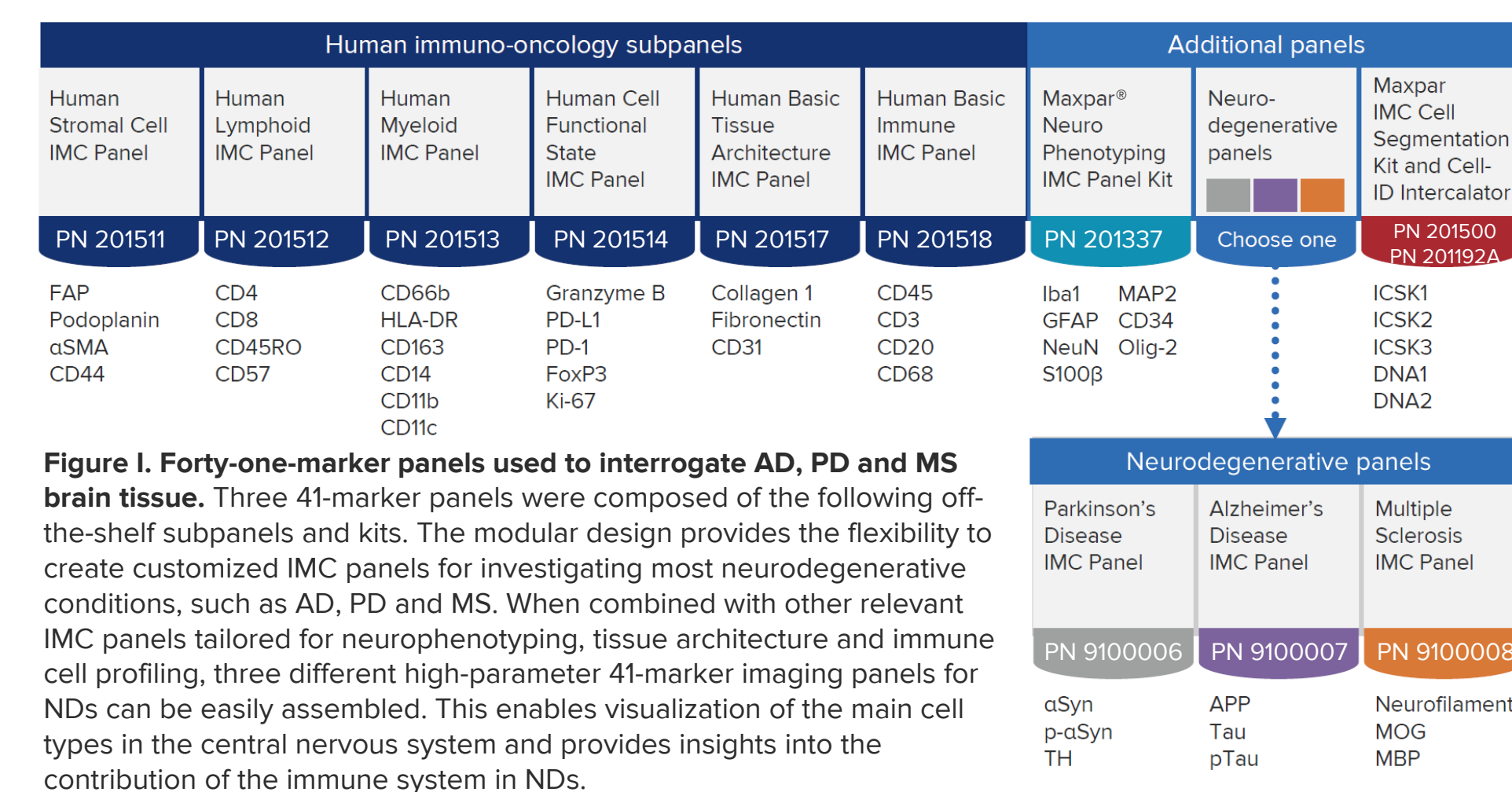
Nick Zabinyakov, Qanber Raza, Thomas D. Pfister, David Howell, Nikesh Parsotam, Liang Lim, Christina Loh, James Pemberton, Jyh Yun Chwee  
Standard BioTools Canada Inc., Markham, ON, Canada

## Abstract

Immune response plays a significant role in the progression of neurodegenerative diseases (NDs) such as Parkinson's disease (PD), Alzheimer's disease (AD) and multiple sclerosis (MS). It is paramount to quantify the immune and structural spatial microenvironment of ND brain using research approaches that resolve tissue at a single-cell level. Imaging Mass Cytometry™ (IMC) is a spatial biology technique that provides quantitative phenotypic evaluation of 40-plus markers. We report the application of IMC imaging modes with a 41-marker panel for ND research. Tissue Mode was applied to perform a scan of the entire tissue followed by pixel-clustering analysis to uncover spatial distribution of relevant markers. Preview Mode was applied to sample the tissue at low resolution, improving informed selection of areas for high-resolution Cell Mode imaging on the same slide. Using Tissue Mode with pixel-clustering analysis, we quantified the spatial distribution of immune cells in tissue compartments of ND tissues. Preview Mode and Cell Mode highlighted MS lesions devoid of myelination and a network of αSynuclein in PD tissue. Single-cell analysis identified heterogeneity of amyloid precursor protein aggregates in AD that encompassed total and phosphorylated species of Tau and phosphorylated αSynuclein. Overall, whole slide imaging techniques using IMC provide quantitative immunological and structural insights into the spatial biology of ND.

## Methods and Materials

Three 41-marker full-configuration IMC antibody panels consisting of modular subpanels and kits (Figure 1) were used to determine the cellular and structural landscape of the three diseased brain tissues. Each panel contained a neurodegenerative subpanel specific to a disease type (AD, PD, MS). We applied these full-configuration panels on the corresponding tissues and identified the spatial distribution of 41 distinct markers. Two open channels were complemented with disease-relevant antibodies from the existing IMC antibody catalog.



We performed imaging using two features of the Hyperion XTI™ Imaging System (Figure 1IA) that provide whole slide scanning capabilities. **Preview Mode** (Figure 1IB, top panel) was applied to rapidly screen tumor cores for expression signatures associated with tumor immuno-oncology processes. This enabled biomarker-guided selection of areas in tumor tissue that were imaged at higher resolution and analyzed using single-cell analysis. In parallel, high-throughput **Tissue Mode** (Figure 1IB, bottom panel) was applied to perform a detailed scan of the whole slide followed by pixel-clustering analysis to unravel the spatial composition of the tissue.

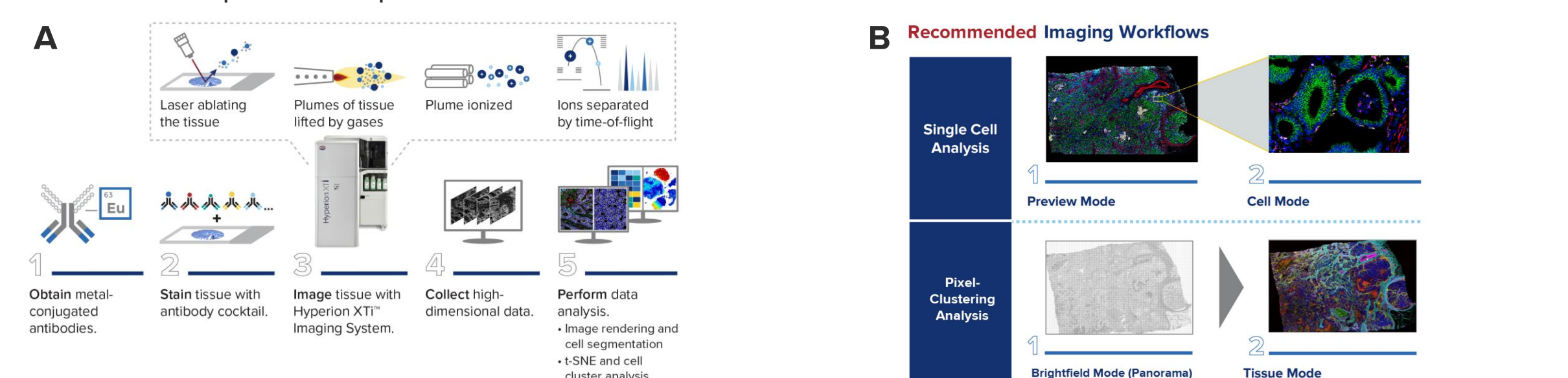


**Figure 2.** Imaging Mass Cytometry workflows. (A) IMC offers a streamlined workflow that simplifies translational and clinical application of multiplexed tissue analysis. The five-step process, which consists of obtaining metal-conjugated antibodies, staining tissues with antibody cocktails, imaging tissues with Hyperion XTI and the collection and analysis of high-dimensional data, can be accomplished in as little as 72 hours for the whole slide. Additionally, the slide loader can accommodate two cassettes of 20 slides each (40 slides total) to greatly increase throughput. (B) The whole slide imaging modes for IMC offer a customized workflow for specific customer needs. Preview Mode offers a rapid scan of the sample and generates useful data for guiding region of interest (ROI) placement for Cell Mode acquisition for single-cell analysis application. Alternatively, Tissue Mode can be applied to generate a high-quality scan of entire tissue sections in a matter of hours with higher spot-size enabling enabling entire tissue analysis using pixel-clustering methods. Both workflows offer unique advantages for specific research requirements.

## Conclusions

Whole slide imaging modes and single-cell and pixel-clustering analysis highlight the power of **Imaging Mass Cytometry** to simultaneously explore numerous **biological outputs** that provide **new perspectives** on the extensive **composition of the neurodegenerative brain**. This enhanced understanding opens avenues for **potential new diagnostic and therapeutic applications**.

## Results

### Preview Mode facilitates rapid tissue screening for ROI selection for Cell Mode imaging

Preview Mode enables quick visualization of all 41 markers within minutes across the whole tissue. This fast scan provides guidance for selecting ROIs to be acquired on the same slide in Cell Mode for single-cell analysis.

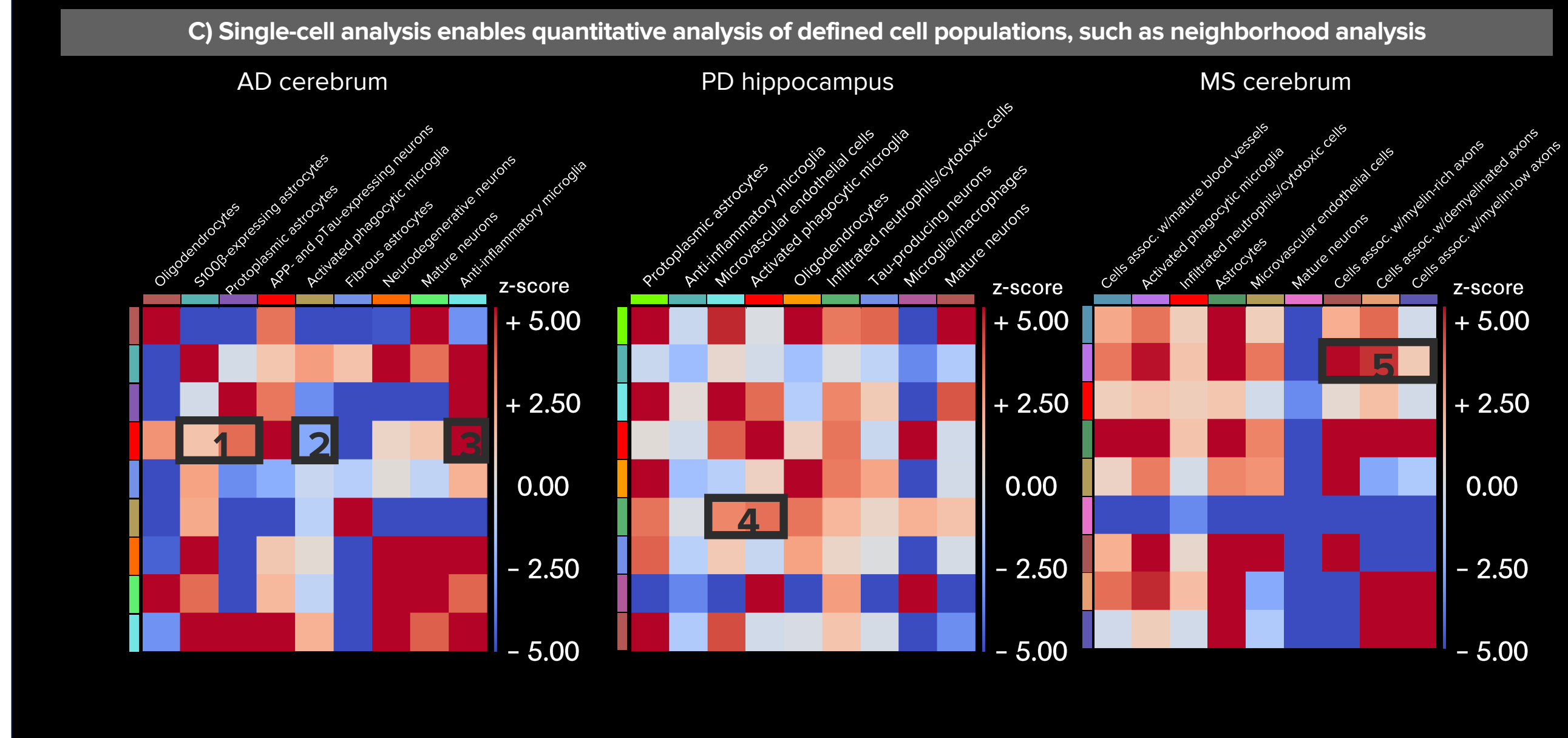
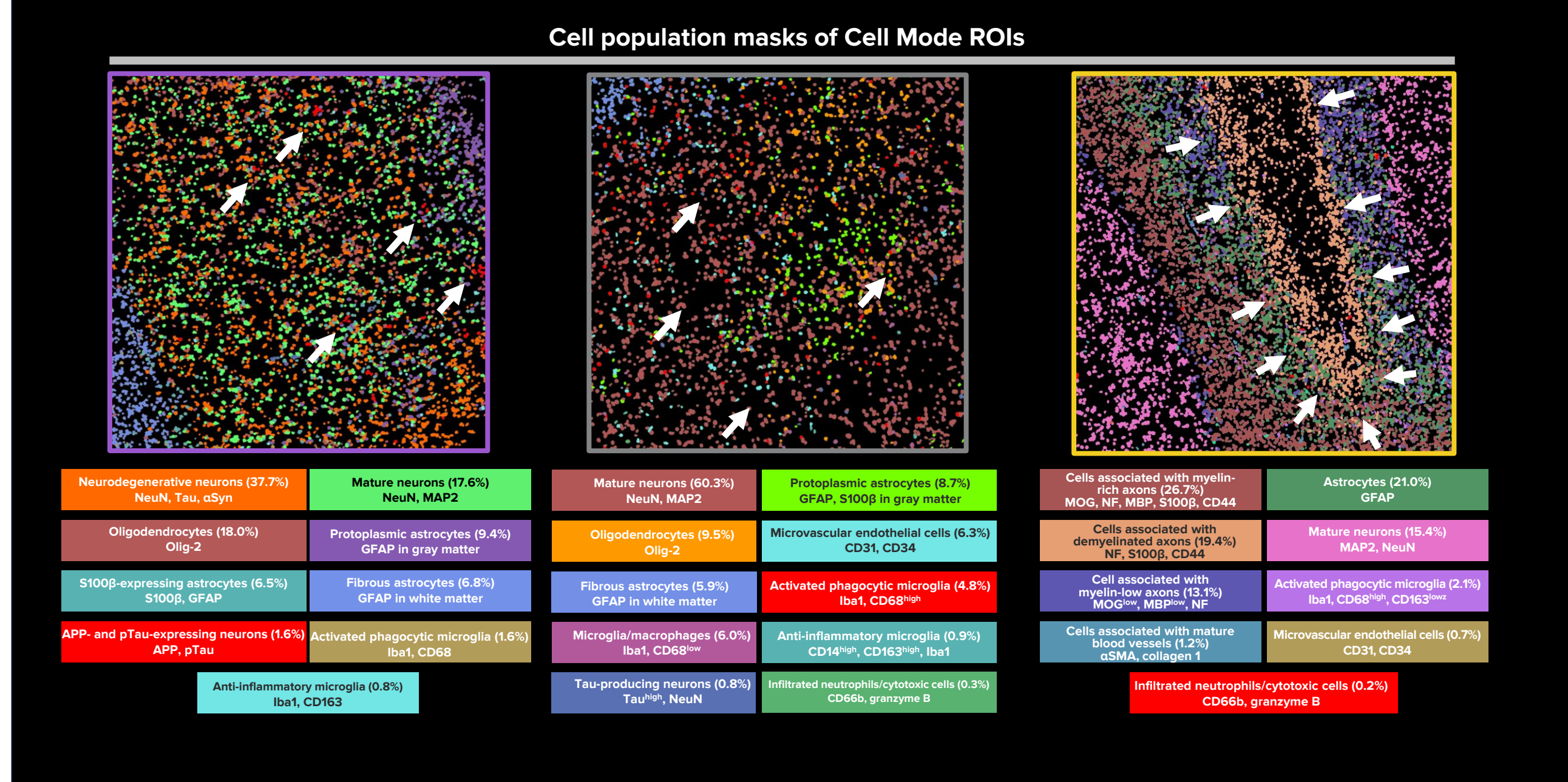
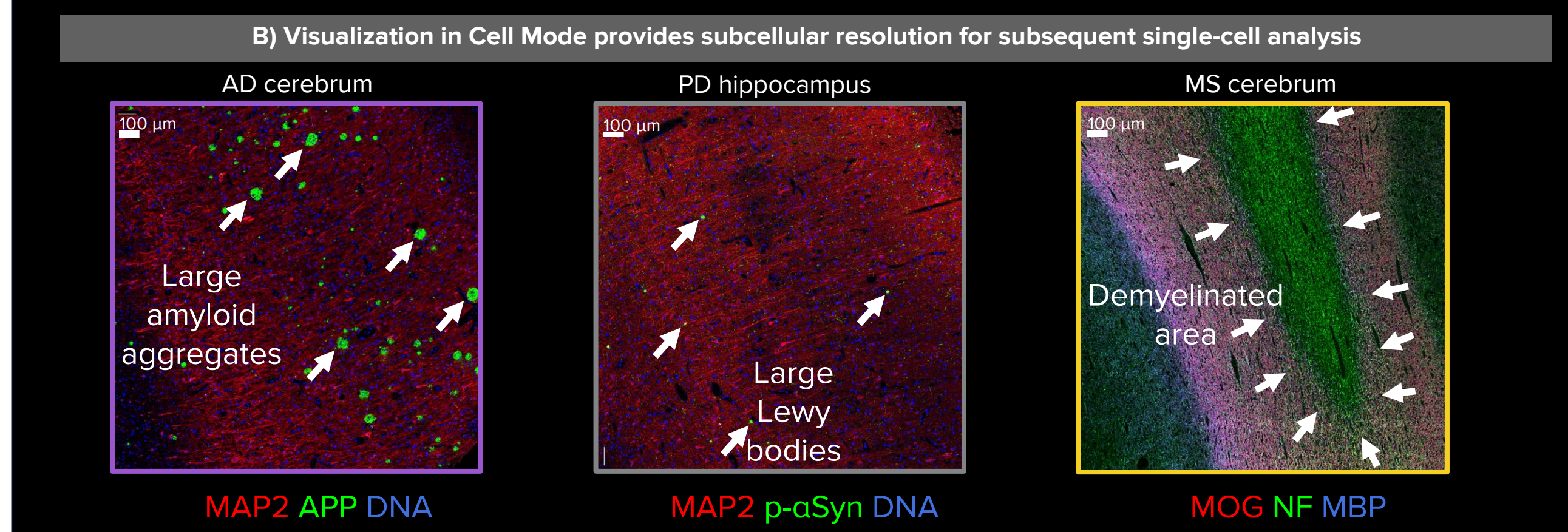
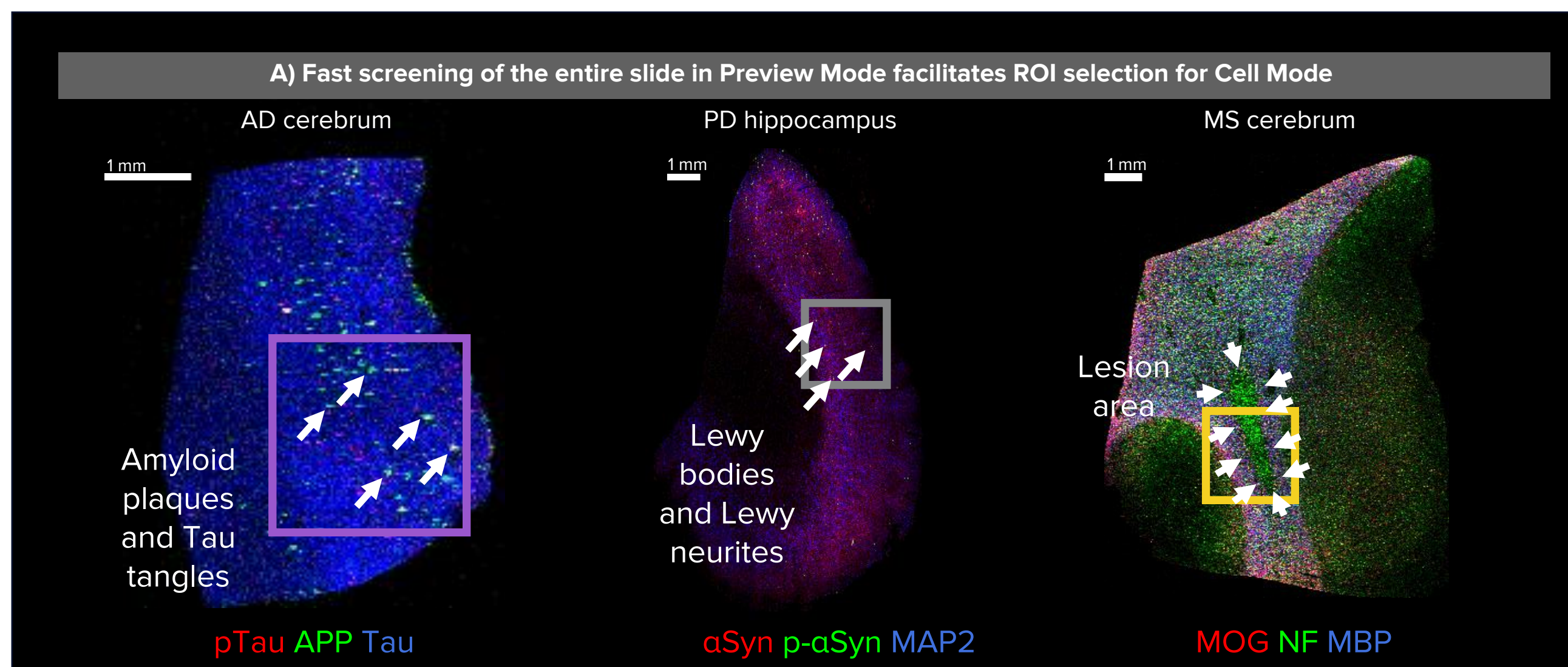


**Figure 1. A) Screening of the whole slide in Preview Mode.** Preview Mode in combination with neurodegenerative panels allow whole tissue visualization of the main protein contributors to disease pathology: amyloid precursor protein (APP) in amyloid plaques and Tau in tangles of AD (left panel); p-αSynuclein (p-αSyn) in Lewy bodies and Lewy neurites of PD (middle panel); and large areas of lost myelin (lesion) in a lesion of MS (right panel). Preview Mode facilitates marker-guided ROI selection for subsequent imaging with Cell Mode.

**B) Visualization in Cell Mode provides subcellular resolution for subsequent single-cell analysis.** Data from Cell Mode acquisition was used to conduct single-cell analysis. Locations of the same aggregates with the most abundant presence of APP and pTau. Lewy bodies and area of demyelination are marked with arrowheads in a Cell Mode image and cell population masks, respectively, for AD, PD and MS. A small population of neurons, 1.5% of all cells, was observed to accumulate high levels of APP and pTau in AD. These neurons tended to localize in the periphery of large aggregates (AD, arrowheads). Significant immune system involvement was not detected in PD: infiltrated neutrophils with cytotoxic properties and activated microglia were not present in the vicinity of Lewy bodies (PD, arrowheads) and instead were distributed in the entire tissue. In MS, three distinct populations of cells associated with the lesion were clearly visible: cells associated with demyelinated axons in the middle and populations of cells associated with myelin-depleted axons in the periphery. Cells associated with myelin-rich axons were located at a distance from the demyelinated area.

**C) Neighborhood analysis of defined cell populations.** Quantitative neighborhood analysis demonstrates heat maps with an enrichment score (z-score) that indicates enrichment or depletion of the spatial proximity between all identified clusters. In AD, aggregate-forming neurons (positive for APP and pTau) were associated with populations of protoplasmic astrocytes and astrocytes expressing elevated levels of S100β thought to promote astrocytic activation (AD, box 1). Neighborhood analysis of AD ROI also suggests a close spatial proximity of aggregate-forming neurons with microglia that exhibit anti-inflammatory properties (AD, box 2), while activated phagocytic microglia appear to be located at a distance (AD, box 3). In PD, infiltrated neutrophils with cytotoxic properties were present adjacent to both blood vessels and activated phagocytic microglia (PD, box 4) suggesting their mediation of microglial response to the spread of the Lewy bodies and Lewy neurites. In MS, activated microglia are present in the vicinity of cell populations associated with demyelinated, myelin-low and myelin-rich axons (MS, box 5). This could indicate that boundaries of demyelination lie beyond the borders of a visible lesion as microglia with phagocytic properties remain active in the lesion periphery. A significant presence of infiltrating immune cells was not observed in MS tissue in selected ROI.

### Tissue Mode highlights pathological tissue compartments in the neurodegenerative brain

Tissue Mode visualizes tissue compartments at a tissue level, facilitating pixel-clustering analysis.

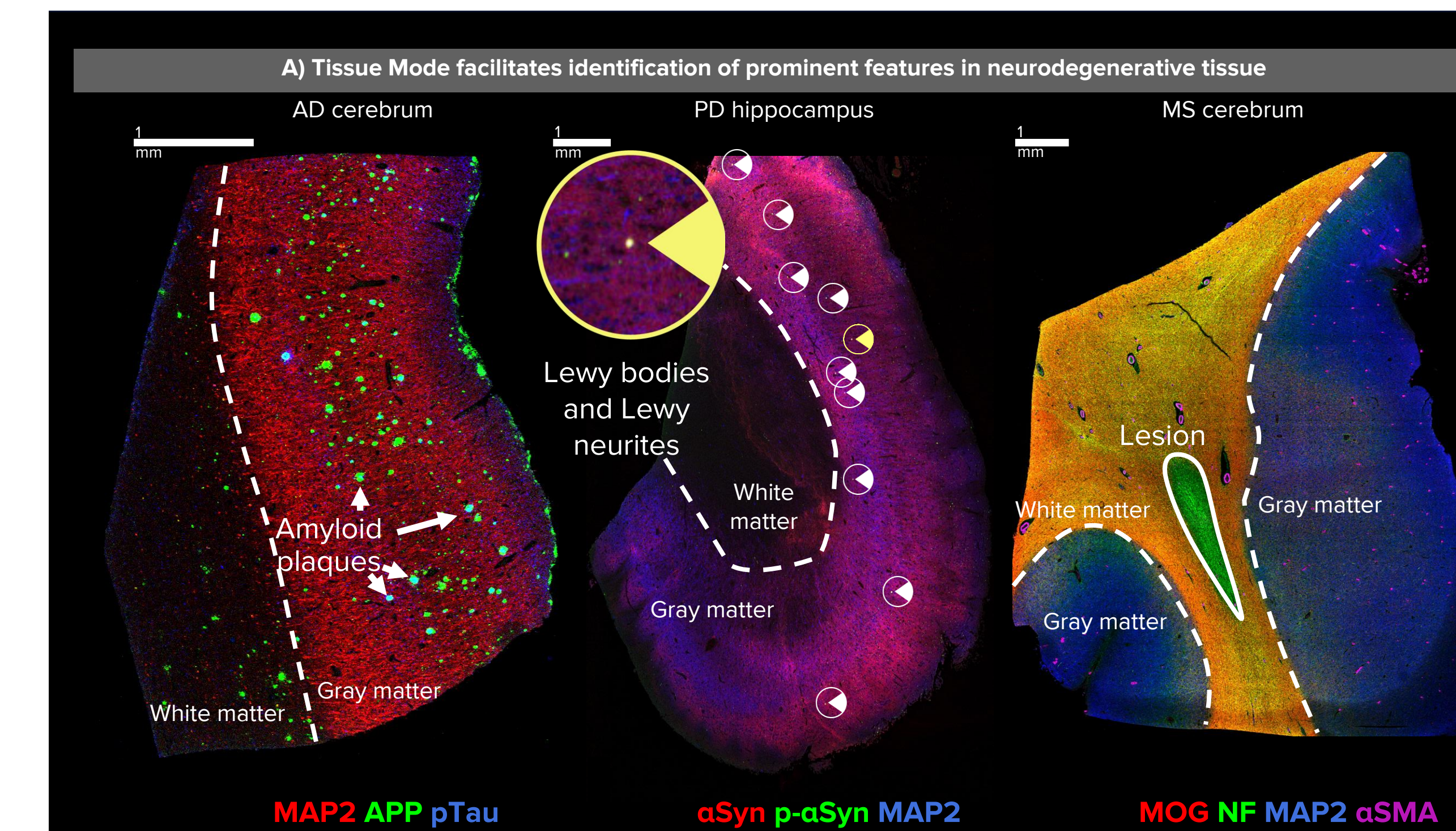


**Figure 2. A) Tissue Mode facilitates identification of prominent features in neurodegenerative tissue.** Similar to Cell Mode, Tissue Mode in combination with neurodegenerative panels allow whole tissue visualization of the main protein contributors to disease pathology: APP in amyloid plaques and Tau in tangles of AD, p-αSyn in Lewy bodies and Lewy neurites of PD, and large areas of lost myelin (lesion) of MS. Whole single-cell analysis provides valuable insights. Nuclei-based segmentation of brain tissue is not sufficient to draw a complete picture of the disease. Additional complex analysis of neuronal, astrocytic and microglial extensions that are not associated with DNA, especially detection of ramified phenotypes, is required to comprehensively understand the cellular population landscape of the diseased brain. Moreover, single-cell analysis is limited in capturing extracellular aggregates because they are devoid of membrane and nucleus markers. Therefore, subsequent pixel-clustering analysis performed on the Tissue Mode ROIs offers a complementary perspective, allowing for the examination of non-nucleated extracellular aggregates and large demyelinated areas at a tissue level.

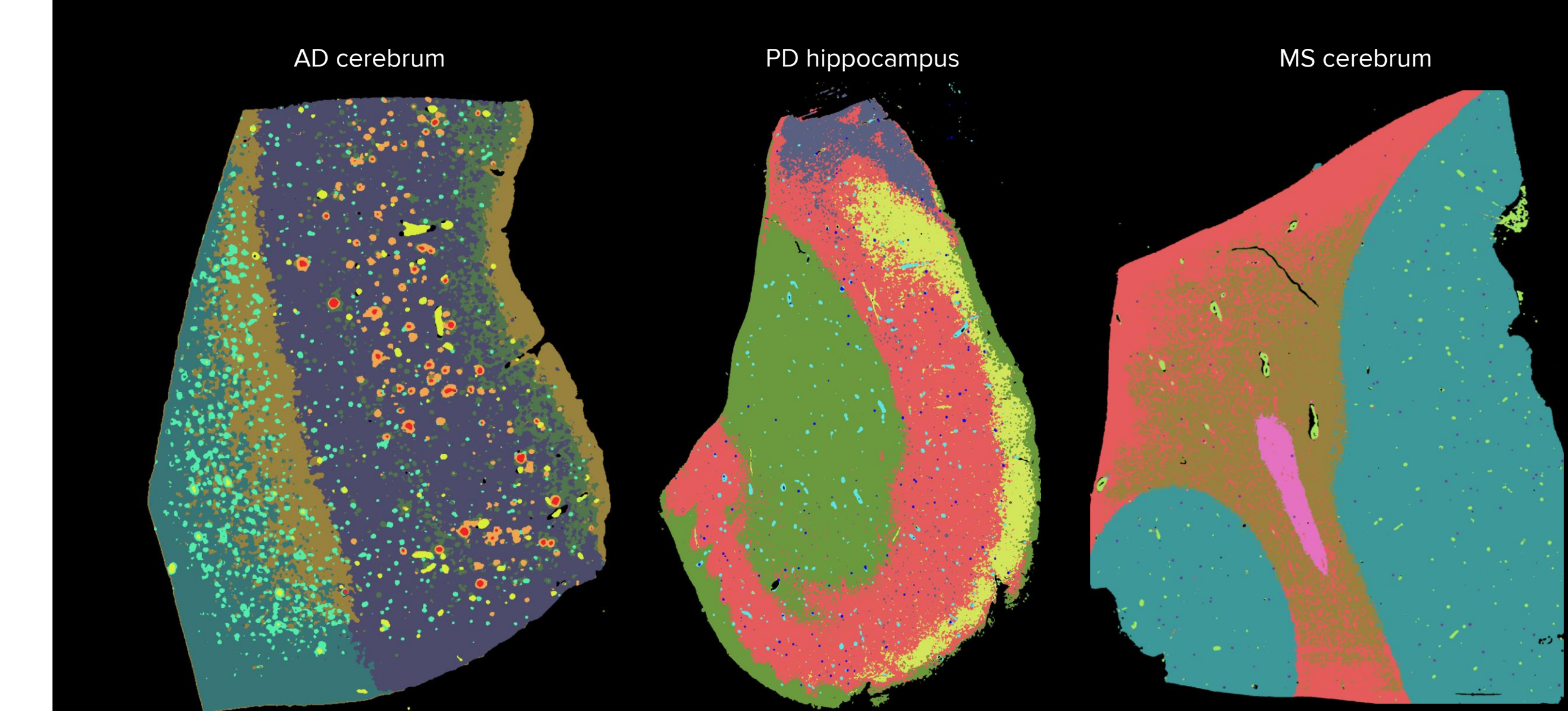
**B) Pixel-clustering analysis of neurodegenerative tissues complements single-cell analysis with additional biological insights.** Pixel-clustering analysis with MOG+ SmartViser software allows for a more unsupervised clustering, which automatically grouped pixels with similar expression pattern by analyzing the intensity and distribution of 41 markers in each pixel.

In AD, pixel-clustering analysis unveiled eight distinct morphology clusters, such as gray matter-associated and white matter-associated microglia (combined in one cluster); three distinct populations of neurons, fibrous and protoplasmic astrocytes (combined in one cluster); oligodendrocytes, and vasculature, alongside the identification of two functional amyloid aggregate clusters. A cluster of neurodegenerative neurons expressing higher levels of Tau and αSyn encompassed a substantial portion of the whole tissue area (53.4% of total analyzed pixels). Aggregates of a relatively small size exhibited an exclusive enrichment of APP, whereas most of the larger aggregates demonstrated a spatial organization characterized by the central concentration of APP surrounded by a halo-like distribution of Tau protein. The arrangement of APP and Tau hints at a potential aggregate stabilization and overall synergy among those proteins, alongside αSyn, all known to be prone to misfolding in the diseased brain.

In PD, the infiltration of immune cells was not seen in this PD sample. However, a small CD68+ microglia/macrophage cluster is seen distributed within the MAP2+ gray matter and MOG+ white matter areas. Other identified clusters were vasculature, mature neurons expressing different levels of Tau protein and a cluster of p-αSyn-producing neurons. As seen in the Tissue Mode image (A, middle panel), the cluster of p-αSyn-producing neurons is spatially associated with the location of Lewy bodies and Lewy neurites.

In MS, three clusters with varying levels of MOG, NF and MBP expression were identified alongside with clusters containing mature neurons, vasculature and microglia/macrophages. The most visually prominent and pathologically relevant cluster identified was composed of demyelinated axons lacking expression of MOG and MBP. The cluster accounted for 17.6% area of the entire tissue. A relatively large cluster (19.3% of total area) of myelin-low axons was present around the lesion, suggesting a progressive loss of myelin in the encircled area. The third cluster of unaffected myelin-rich neurons surrounded the first two and incorporated 18.6% of the total visualized area.

### Pixel-clustering analysis of neurodegenerative tissues complements single-cell analysis with more biological insights



Neurodegenerative neurons (53.4%) NeuN, MAP2, Tau, αSyn	Mature neurons (58.4%) NeuN, MAP2, Tau <sup>high</sup>	Mature neurons (58.4%) NeuN, MAP2, Tau
S100β-expressing glia (19.3%) GFAP, S100β, Olig2	White matter (39.0%) MOG, CD44, podoplanin	Myelin-low axons (19.8%) MOG <sup>low</sup> , MBP <sup>low</sup> , NF
Fibrous and protoplasmic astrocytes (17.8%) GFAP, CD44, αSyn	Mature neurons (10.3%) NeuN, MAP2, Tau <sup>low</sup>	Myelin-rich axons (18.6%) MOG, MBP, NF
Tau-producing neurons (9.7%) Tau, pTau, αSyn, MAP2	p-αSyn-producing neurons (5.7%) αSyn, p-αSyn, MAP2	Demyelinated axons (17.6%) NF, S100β
Gray and white matter-associated microglia (6.0%) Iba1, CD68, αSyn, MAP2, CD44	Vasculature (1.8%) αSMA, CD31, CD34	Vasculature (1.1%) αSMA, collagen 1
APP-producing neurons (2.8%) APP, MAP2, NeuN	Microglia/macrophages (0.4%) Iba1, CD68	Microglia/macrophages (0.3%) Iba1, CD68
APP- and pTau-containing aggregates (0.4%) APP, pTau	Vasculature (1.5%) CD31, collagen 1, αSMA, CD34	

